Temperature-dependent polarization effects in Ce:LiLuF

Andrew J. S. McGonigle, Richard Moncorgé, and David W. Coutts

We report on tuned-laser, pump–probe-gain, and fluorescence yield studies of the effect that crystal temperature plays on the polarized emission characteristics of Ce:LiLuF. It was found that σ-polarized emission at the 327-nm fluorescence spectra peak is characterized by smaller laser pulse buildup times, higher small-signal gains, and smaller output powers than the π-polarized 327-nm emission. We concluded that excited-state absorption (ESA) (and the resultant formation of color centers) is more severe for σ-polarized emission than for π-polarized emission in this spectral region. We postulate that the enhancement in laser performance and crystal fluorescence observed with crystal cooling is due to narrowing of the ESA absorption band that reduces the probability of ESA and color-center formation.

OCIS codes: 140.0140, 140.3320, 140.3610, 140.3580, 140.6810.

1. Introduction

Ultraviolet lasers, tunable around the 300-nm spectral region, are extremely important tools for applications such as lidar and combustion diagnostics. A wide range of methods exists for generating tunable UV laser output, such as use of optical parametric oscillators or nonlinear frequency conversion of dye lasers and titanium sapphire lasers. An attractive alternative mechanism is the use of solid-state cerium-doped-fluoride lasers that are directly tunable in the 280–340-nm spectral region. Not only do cerium lasers offer the convenience of spectral manipulation in the wavelength region of interest but they are also relatively simple and compact compared with the alternative, tunable UV laser generation techniques.

In the past few years, cerium lasers have been developed that have impressive performance characteristics; with output powers as great as 550 mW,[1] tuning ranges as broad as 35.5 nm,[2] pulse energies as high as 27 mJ,[3] and slope efficiencies as great as 55%.[4] However, earlier attempts to realize laser operation in trivalent cerium-doped materials on the interconfigurational $5d \Rightarrow 4f$ transition were considerably less successful.[5–8] Before 1992 only two[9,10] of the many cerium-doped media investigated were found to be laser active. This disappointing behavior was attributed to the coupled effects of excited-state absorption (ESA) and absorption that is due to the formation of color centers. These two effects are particularly acute in the UV cerium laser scheme owing to the relatively high pump and laser photon energies, and it is now recognized that some combination of these loss mechanisms plays a deleterious role in the operation of all cerium-doped laser materials.

Until recently, more attention has been focused on Ce:LiCAF (Ref. 11) and Ce:LiSAF (Refs. 12 and 13) than on Ce:LiLuF,[14,15] owing to the mature crystal growth procedures developed for Ce:LiSAF and Ce:LiCAF as well as the ready availability of pump sources for the former media in the form of frequency-quadrupled Nd^{3+} lasers. Ce:LiLuF has three major pump absorption bands that are centered at 210, 245, and 290 nm, and in the past Ce:LiLuF lasers have been pumped at 248 mm by KrF excimer lasers[3,14,15] as well as at 213 nm by a frequency-quintupled Nd:YAG laser.[16] However, the most efficient Ce:LiLuF lasers reported to date have all used longer wavelength pump sources in the forms of a frequency-quadrupled Nd:YAG laser pumped Ce:LiSAF laser that operates at 290 nm (Ref. 4) and a 289-nm frequency-doubled copper vapor laser (CVL).[17,18] By

When this research was performed, A. J. S. McGonigle and D. W. Coutts were with the Oxford Institute for Laser Science, Department of Atomic and Laser Physics, Clarendon Laboratory, Parks Road, Oxford OX1 3PU, UK. A. J. S. McGonigle (ajsm2@cam.ac.uk) is now with the Department of Geography, University of Cambridge, Downing Place, Cambridge CB2 3EN, UK. R. Moncorgé is with the Centre Interdisciplinaire de Recherche Ions Lasers, Unite Mixte de Recherche 6637, Commissariat a l'Energie Atomique, Centre National de la Recherche Scientifique, Institut des Sciences de la Matiere et du Rayonnement, Universite de Caen, 14050 Caen Cedex, France.
Received 4 December 2000.
0003-6935/01/244326-08$15.00/0

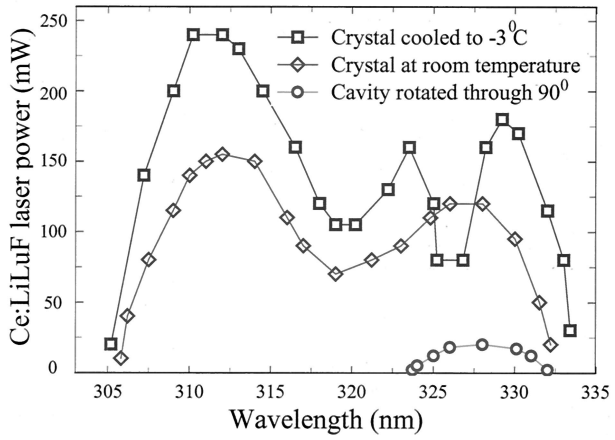

Fig. 1. Prism-tuned Ce:LiLuF laser output power versus wavelength, when the crystal was at −3 and at 25 °C. The tunability of the laser about the 327-nm peak in the fluorescence spectrum is also shown, when the laser cavity was rotated by 90° and the crystal was cooled to −3 °C.

pumping into the first absorption band, we have reduced ESA-related problems leading to the highest average output power (380 mW) yet achieved from a Ce:LiLuF laser.[17] Additionally, when Ce:LiLuF crystals of very high quality were used to reduce the probability of color-center formation, the most efficient (55% slope efficiency) report of a Ce:LiLuF laser to date[4] as well as the first report, to our knowledge, of continuous tunability across both peaks (311 and 327 nm) in the tuning curve were obtained. These recent studies have demonstrated that Ce:LiLuF, when operated in the right conditions, is a more efficient laser material than the better known Ce:LiCAF and Ce:LiSAF, and therefore that Ce:LiLuF should merit more attention as a practical tunable UV laser source for applications in which, as yet, Ce:LiCAF and Ce:LiSAF have been the only utilized cerium lasers.[19]

Recently we reported on the continuous tunability of a frequency-doubled CVL-pumped Ce:LiLuF laser across both peaks in the tuning curve[18] from 305 to 333.2 nm, as shown in Fig. 1. By cooling the cerium laser crystal from room temperature to −3 °C, we found that the laser output power increased at all tuning wavelengths, except in the vicinity of the fluorescence spectra peak at 327 nm, where the laser power decreased. It is interesting that when the crystal was cooled the laser oscillation in this spectral window became progressively more σ polarized, although oscillation at all the other tuning wavelengths was π polarized, in accordance with the orientation of the intracavity Brewster-cut prism that was used to obtain wavelength selectivity. In another study[17] we reported on passive absorption of a 633-nm He–Ne laser beam that was due to color centers in the pumped region of a Ce:LiLuF crystal. We found this absorption to be more pronounced in σ polarization than in π polarization and to be virtually eliminated by cooling the crystal to −3 °C. It was also shown in this study that use of an additional σ-polarized anti-

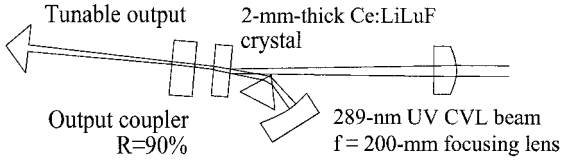

Fig. 2. Experimental configuration for the prism-tuned Ce:LiLuF laser.

solarant pump beam, for bleaching the color centers, led to a 30% increase in the Ce:LiLuF laser pulse amplitude. Indeed, it is believed that the effects of ESA and color-centre formation in Ce:LiLuF are more accentuated in σ polarization than in π polarization in the 300-nm spectral region, in common with Ce:LiCAF and Ce:LiSAF.[12] However, before we presented the study in this paper, this point had not been proved.

Here we present results of further experiments that build on our earlier observations investigating in more detail the effect that temperature plays on the polarization characteristics of the Ce:LiLuF laser. In particular, additional laser experiments as well as studies of small-signal gain and investigations into the effect of temperature on the crystal fluorescence yield are documented. The results of these inquires provide novel insights into the roles that color centers and ESA play in the laser kinetics of Ce:LiLuF.

2. Laser Experiments

A. Experimental Configuration

The pump source[20,21] used in all the experiments reported in this paper was a frequency-doubled CVL operated at the 289-nm harmonic of the 578-nm CVL yellow line. This laser provided as much as 920 mW of output power at a pulse repetition frequency (PRF) of 10 kHz with a 7-ns FWHM pulse length. A more thorough description of the configuration of this laser has appeared elsewhere.[17] An uncoated plane-cut 2-mm-thick Ce:LiLuF crystal was used. It was grown by use of the Czochralski technique at the Université du Maine. The crystallographic *c* axis was contained in the plane of the end faces, and a π-polarized pumping configuration was adopted so that 95% of the 289-nm pump beam was absorbed in the crystal. A brass mount that could be cooled to −3 °C was used to cool the crystal conductively.

The basic Ce:LiLuF laser cavity arrangement used in the experiments described here is shown in Fig. 2. The arrangement is the same as was used to obtain the tuning curves shown in Fig. 1[18] This 65-mm-long cavity consisted of a flat output coupler with reflectivity of 90% at the Ce:LiLuF laser wavelengths, a fused-silica Brewster-cut prism, and a curved (250-mm radius of curvature) high reflector. The pump beam was focused past the prism, with an f = 200-mm lens used to form a 200-μm-diameter focus in the crystal, which matched the cavity mode size. A quasi-longitudinal pumping geometry was adopted owing to the difficulty of manufacturing a

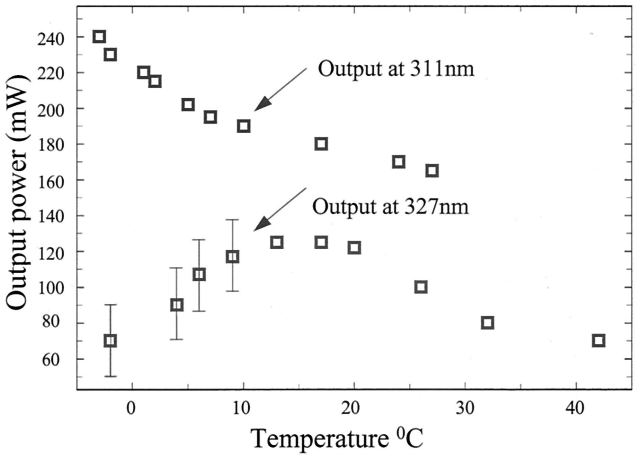

Fig. 3. Ce:LiLuF laser output power versus crystal temperature when the laser was tuned to 311 and 327 nm.

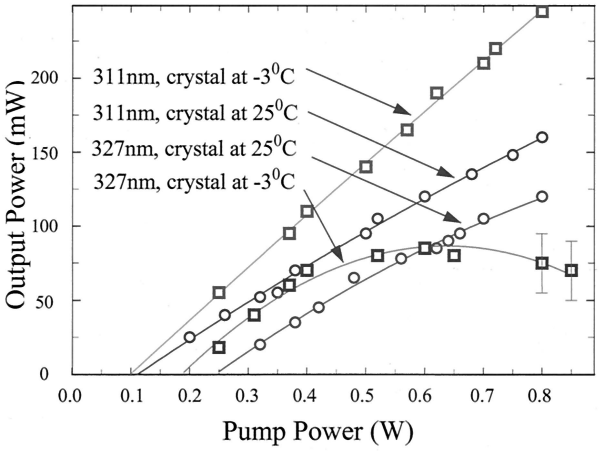

Fig. 4. Ce:LiLuF laser output power versus pump power when the laser was tuned to 311 and 327 nm, when the Ce:LiLuF crystal was at −3 and at 25 °C.

dichroic mirror coating of high reflectivity at the laser wavelengths and high transmission at the pump wavelength with a sufficiently high damage threshold. This cavity was oriented in a plane so that the π-polarized oscillation was favored, owing to the relative magnitudes of the polarized Fresnel losses at the Brewster prism faces.

B. Results

The output powers versus crystal temperature from the Ce:LiLuF laser, when tuned to the 311- and 327-nm peaks in the tuning curve, are shown in Fig. 3, when this laser was pumped with 800 mW. While the 311-nm laser output power increased monotonically as the crystal was cooled, the output at 327 nm only increased down to a temperature of around 15 °C. Below this temperature the 327-nm output power decreased with decreasing temperature. In this lower temperature region the 327-nm output power fluctuated considerably (±20 mW at −3 °C), becoming increasingly σ polarized as the temperature was reduced, as evidenced by enhanced Fresnel reflections from the Brewster prism (15–35 mW at −3 °C). The 311-nm output was almost completely π polarized for all temperatures, as was the 327-nm output above 15 °C.

Plots of the output power at 311 and 327 nm versus pump power are shown in Fig. 4, both when the crystal was at room temperature (25 °C) and at −3°C. At −3 °C the 311-nm output increased linearly with pump power, with a slope efficiency of 35%. At room temperature the 311- and 327-nm outputs were found to saturate slightly at higher pump powers, with a slope efficiency of 25% before saturation in both cases. When the laser crystal was cooled to −3 °C the 327-nm output increased linearly with pump power with a slope efficiency of 35% before saturation and roll-off. Above 600 mW of pump power the 327-nm output power fluctuated considerably, becoming progressively more σ polarized with increased pump power. At lower pump powers the 327-nm output was almost completely π polarized when the crystal was cooled to −3 °C, as was the output in all the other temperature, wavelength, and pump power conditions in Fig. 4.

When the laser was tuned to 327 nm the laser pulse shapes and crystal fluorescence depletions were studied for both −3 and 25 °C crystal temperatures, as shown in Table 1 and Fig. 5 (note that Fig. 5 contains only the laser pulse shapes). It is interesting that, when the cerium crystal was at −3 °C, it was evident that the fluctuating output power described above was caused by two competing modes of operation, as shown in Fig. 5. It was demonstrated with a polarizing cube that these modes were σ and π polarized and that the former mode was characterized by shorter buildup times and pulse lengths as well as smaller pulse amplitudes.

It was found that there was visible fluorescence evident in the laser mode of the crystal as the laser was tuned across discrete wavelength intervals within the 315.5–332-nm spectral range for both

Table 1. Pulse Shape Data for the Ce:LiLuF Laser Tuned to 327 nm[a]

Crystal Temperature (°C)	Pump Power (mW)	Pulse Length (ns)	Buildup time (ns)	Laser Polarization	Fluorescence Depletion (%)
25	670	4.9	12.6	Mostly π	65
−3	750	2.5/(4.9)	8.2/(10)	σ/(π)	48 (mean)

[a]Note the competing polarized modes of operation when the crystal was cooled to −3 °C.

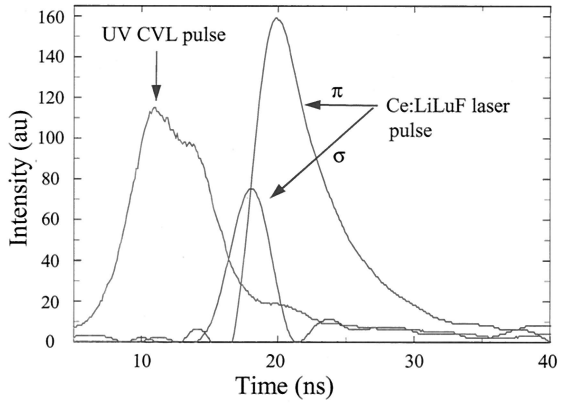

Fig. 5. Pulse shapes of the competing polarized modes of operation when the Ce:LiLuF laser was tuned to 327 nm and crystal was cooled to −3 °C.

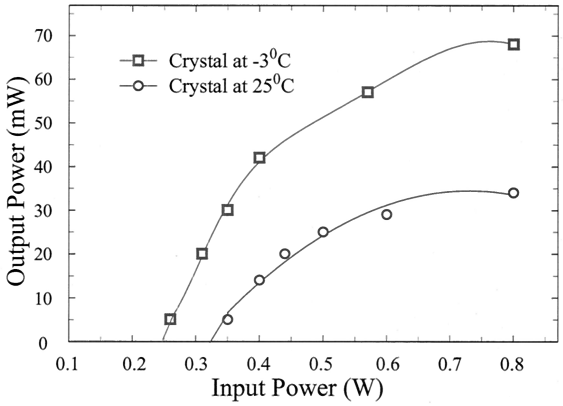

Fig. 6. Output power of 327.5 nm versus input power when the Ce:LiLuF laser was implemented with the output coupler that forced lasing to occur in the vicinity of the 327-nm peak in the emission spectrum, without imposing any polarization bias on the oscillation.

−3 °C and room-temperature crystal conditions. The color of the fluorescence varied from interval to interval, and when the crystal was cooled below 15 °C, so that the σ-polarized lasing was enhanced when the laser was tuned in the 325.5–329-nm spectral range, the visible fluorescence was correspondingly enhanced across this tuning range. This fluorescence was not evident in the presence of the π-polarized pump beam alone and neither intensified with time nor persisted after the lasing was blocked.

Additional laser experiments were performed by rotating this laser cavity (but not the crystal) through 90° so as to favor σ-polarized oscillation. The tunability of this orthogonal cavity Ce:LiLuF laser, about the 327-nm fluorescence peak, is shown in Fig. 1 when the crystal was cooled to −3 °C and pumped with 640 mW. In these conditions tunability was attained from 323.5 to 332.5 nm, and 35 mW was derived from the laser at 327 nm. The pulse buildup time was measured to be 8.7 ns, and the crystal fluorescence was depleted by 65% by the laser mode when the laser was operated at 327 nm. When the Ce:LiLuF crystal was at 25 °C only 20 mW of 327-nm output power was obtained from the laser, from 640 mW of pump power, and the tunability was reduced slightly to 323.7–332 nm. The fluorescence depletion on lasing was 55%, and the pulse buildup time was 10 ns for 327-nm lasing. In both of these crystal temperature conditions the laser output was σ polarized.

A third laser cavity was investigated, in which the prism was removed and the output coupler was replaced with a flat mirror that was 70% reflecting at the longer-wavelength fluorescence peak, but only 30% reflecting at the shorter-wavelength fluorescence peak, where free lasing would normally occur in the absence of wavelength-selective elements. This arrangement was implemented in an attempt to force the lasing to occur in the spectral vicinity of 327 nm without imposing polarization bias on the cavity.

The output powers versus input power for this laser are shown in Fig. 6, when the crystal was operated at both −3 and 25 °C. In this cavity geometry the laser oscillation was at a wavelength of 327.5 nm and was almost completely σ polarized, with strong saturation evident above pump powers of 400 mW. When this laser was pumped with 800 mW, output powers of 70 and 35 mW were derived at crystal temperatures of −3 and 25 °C, respectively. The pulse buildup time was found to be 11.8 ns, and the crystal fluorescence was depleted by 50% by the laser mode when the crystal was operated at 25 °C, and 700 mW of pump power was applied. In the same pumping condition the pulse buildup time was decreased to 10 ns, and the Ce:LiLuF fluorescence was depleted by 57% by the laser mode when the crystal was cooled to −3 °C. It is interesting that, when a Brewster prism was placed in this cavity, to ensure that most of the laser output was in the π polarization, 140 mW of output power was derived at 327 nm from 670 mW of pump power when the crystal temperature was −3 °C.

3. Further Experiments

We performed small-signal gain measurements by using the frequency-doubled output of a 10-kHz PRF Nd:YLF-pumped dye laser as a probe source. The probe laser was tuned to either 309 or 327 nm to measure the Ce:LiLuF crystal single-pass gain in the spectral vicinity of the two tuning curve peaks. The time delay between the probe pulse and the 289-nm pump pulse was adjusted to maximize the recorded gain value by use of a digital delay generator, and the probe beam was attenuated so as to minimize perturbation of the cerium laser level populations. We focused both the pump and the probe beams colinearly into the Ce:LiLuF crystal by using an f = 100-mm lens to form a pump spot size of ~100 μm, with the focused probe diameter being sufficiently small so as to interrogate only the uniform central region of the pumped volume. The results of these gain experiments are shown in Table 2 for both the −3 and 25 °C crystal conditions,

Table 2. Small-Signal Single-Pass Gain ($G = I_{out}/I_{in}$) in the Ce:LiLuF Crystal[a]

Values	Gain	
	G π	G σ
309 nm		
Crystal at −3 °C	36	6
Crystal at room temperature	24	4.2
327 nm		
Crystal at −3 °C	3.6	5.2
Crystal at room temperature	3.1	4

[a]For 309- and 327-nm probe wavelengths and both −3 and 25 °C crystal temperatures when the crystal was pumped with 500 mW.

when the cerium crystal was pumped with 500 mW of pump power.

Finally, the variation of the Ce:LiLuF crystal fluorescence pulse shape with pump fluence and crystal temperature was investigated. Figure 7 shows the crystal fluorescence transients when this crystal was at room temperature and at 10 °C, both when the 500-mW pump beam was focused into the crystal with an $f = 100$-mm lens and when the pump beam was unfocused. The fluorescence was viewed from the side of the crystal and thus consisted of purely σ-polarized emission. At both temperatures the fluorescence profile when the pump laser was focused into the crystal displayed a lower peak value and a faster decay rate than the corresponding profile when the pump beam was unfocused. The crystal fluorescence yield was greater at 10 °C than at room temperature for both the focused and the unfocused pump arrangements, and by imaging the fluorescence into a monochromator we validated that the fluorescence increased at both the 327- and the 309-nm wavelengths when the crystal was cooled. By multiplying by a factor of 1.3 the pulse shapes taken when the crystal was at 25 °C, we obtained an exact match to the pulse shapes recorded when the crystal was at 10 °C for both the focused and the unfocused pumping configurations.

The ratio of the magnitude of the crystal fluorescence pulse shapes when the crystal was cooled to 6 °C versus when the crystal was at 25 °C was greater when the fluorescence was viewed from the side (1.5) of the crystal (and thus consisted of purely σ-polarized emission) than when the fluorescence was viewed from the crystal end (1.38) (containing both σ- and π-polarized components). The fluorescence lifetime of the Ce:LiLuF crystal was unchanged within the temperature range of −3–40 °C.

4. Discussion

In Sections 1–3 the results of a number of experiments designed to investigate the temperature-dependent polarization behavior of Ce:LiLuF lasers have been outlined. When the Ce:LiLuF laser was operated with an output coupler than ensured oscillation around the 327-nm fluorescence spectra peak, twice the output power was derived from this laser when it was operated with an intracavity prism that ensured π-polarized lasing than when it was operated without this prism and the lasing was σ polarized. Additionally, by comparing orthogonal configurations of the prism-tuned cavity with the $R = 90°$ output coupler, which favored either σ- or π-polarized oscillation, it was found that the 327-nm output power derived from a given pump power was always considerably greater in the π polarization (see Fig. 1). It is interesting, however, that, when this laser cavity was rotated to favor σ-polarized oscillation, the fluorescence depletion (65%) by the laser mode was greater than that recorded for the π-polarized cavity arrangement.

It is also surprising that when the pulse shape data are examined for the competing σ- and π-polarized modes, shown in Fig. 5 and Table 1, as well as for the orthogonal cavity configurations with the $R = 90\%$ output coupler, for equivalent pump powers, it is found that pulse buildup time is always less for σ-polarized lasing than for π-polarized operation. This result correlates well with the fact that the 327-nm emission cross section is greatest for the σ polarization[4] as well as with our finding that the 327-nm small-signal gain was greater in the σ than in the π polarization. Indeed, when the Ce:LiLuF laser was implemented with the prismless cavity that ensured oscillation in the vicinity of 327 nm with no polarization selectivity, the laser oscillated in the σ polarization.

These anomalous results must imply one or both of the following. First, a loss mechanism (such as color centers) that is more pronounced for σ-polarized 327-nm lasing could develop as the intracavity laser field is amplified. Second, ESA effects that are more severe in the σ polarization at 327 nm could cause the population inversion to deplete more rapidly as the laser field grows, reducing the available power for the laser pulse to extract. These two postulates are supported by the observation of strong saturation in the σ-polarized 327.5-nm output shown in Fig. 6, in contrast to the negligible saturation demonstrated by all the π-polarized lasers reported here.

More insight into these results can be gained from Eq. (1), which describes the relationship between the polarized small-signal gains $G_{\pi,\sigma}$, the number density of the $5d$ level and color centers, N_{5d}, N_{CC}, and the polarized emission, ESA, and color-center absorption cross sections at the probe wavelength; $\sigma_{EM}(\lambda_{\mathrm{PROBE}})_{\pi,\sigma}$, $\sigma_{\mathrm{ESA}}(\lambda_{\mathrm{PROBE}})_{\pi,\sigma}$, and $\sigma_{CC}(\lambda_{\mathrm{PROBE}})_{\pi,\sigma}$ for a crystal of length d:

$$G_{\pi,\sigma} = \exp\left\{\int_0^d (N_{5d}(z)[\sigma_{EM}(\lambda_{\mathrm{PROBE}})_{\pi,\sigma} - \sigma_{\mathrm{ESA}}(\lambda_{\mathrm{PROBE}})_{\pi,\sigma}] - \sigma_{CC}(\lambda_{\mathrm{PROBE}})_{\pi,\sigma} N_{CC}(z))\mathrm{d}z\right\}. \quad (1)$$

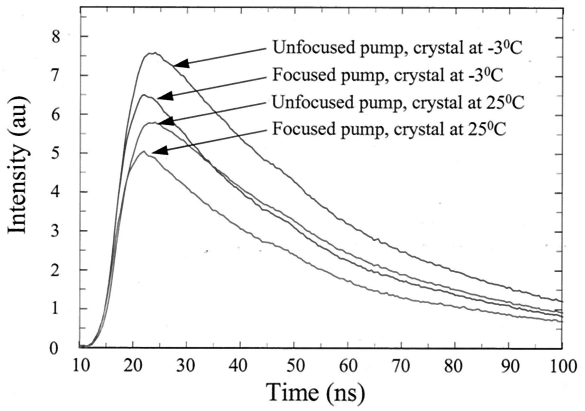

Fig. 7. Fluorescence pulse shapes from the Ce:LiLuF crystal taken when the crystal temperature was −3 and 25 °C as well as for focused and unfocused pumping conditions.

Therefore, in the absence of ESA and color-center losses, $\log G_{\pi,\sigma}$ should be directly proportional to the polarized emission cross section. When data from the small-signal gain shown in Table 1 are used, values of 0.5 and 1.25 are derived for $\log G_{\sigma}/\log G_{\pi}$ at the 309- and 327-nm wavelengths. However, values of 1.1 at 309 nm and 2.4 at 327 nm for $\sigma_{EM}(\lambda_{\mathrm{PROBE}})_{\sigma}/\sigma_{EM}(\lambda_{\mathrm{PROBE}})_{\pi}$ are obtained from the polarized emission spectra of Ce:LiLuF,[4] indicating that the net loss that is due to ESA and the color centers is considerably more pronounced in the σ polarization than in the π polarization. This is supported by the observation of an enhancement in the visible fluorescence related to the color centers in the crystal when the laser oscillation contained a significant component of σ-polarized oscillation, despite the fact that this fluorescence was not evident in the presence of the π-polarized pump beam alone. Indeed, in the past we have demonstrated that the absorption of a 633-nm He–Ne laser owing to color centers is stronger in the σ than in the π polarization.[17]

Cooling the laser crystal also had a greater effect on the σ-polarized behavior of the Ce:LiLuF laser than the π-polarized behavior. For example, the σ-polarized 327-nm laser output shown in Fig. 6 was increased by 100% by cooling from 25 to −3 °C. Yet the π-polarized 309-nm output shown in Fig. 1 increased by only 55% after cooling by this amount. Similarly, the σ-polarized crystal fluorescence viewed from the crystal side increased by a larger factor (1.5) than the mixture of σ- and π-polarized fluorescence viewed from the end of the crystal (1.38) when the crystal was cooled from room temperature to 6 °C.

To account for these results, and particularly for the observation that the ratio of the fluorescence values for the cold versus the hot crystal was invariant of whether the pump beam was focused into the crystal (Fig. 7), it is proposed that these temperature effects are mediated by a simple one-photon process involving fluorescence photons. Given that the onset of the $5d \Rightarrow$conduction band energy occurs at ~390 nm in Ce:LiLuF,[22] it is postulated that the fluorescence photon energies correspond to the low-energy tail of this ESA feature so that this transition is narrowed after cooling so that the probability of ESA is reduced significantly. It is also proposed that the $5d \Rightarrow$conduction band energy is smaller perpendicular to the *c* axis than it is parallel to this axis, which explains why a reduction in crystal temperature has more pronounced consequences for ESA and color-center effects in the σ polarization than in the π polarization. It has been suggested that the ESA effects observed in Ce:LiSAF and Ce:LiCAF, which are more severe in the σ polarization than in the π polarization, arise from layered crystal structures that result in the $5d \Rightarrow$conduction band energies being less perpendicular to the *c* axis than parallel to the *c* axis.[12]

The above hypotheses are also based on a number of other considerations. First, ESA has been observed when Ce:YLF (which is nearly structurally and spectrally identical to Ce:LiLuF) was pumped by a 308-nm XeCl laser,[23] implying that ESA is likely to occur in Ce:LiLuF in the 300-nm spectral region. Second, the Ce:LiLuF fluorescence lifetime did not change across the studied temperature range (−3–40 °C), indicating that crystal heating does not lead to the introduction of an alternative 5*d* level relaxation mechanism. Third, the reduction in crystal temperature has already been shown to lead to increased Ce:YLF color-center lifetimes through reduced thermal deactivation,[24] implying that enhancement in the performance of our Ce:LiLuF lasers at colder temperatures is not related to a color-center depletion process. Indeed we postulate that our previous observation of a reduction in color center induced absorption of a 633-nm probe beam with crystal cooling was caused by a decrease in the rate of the color center forming ESA transition. These temperature-dependent effects could be analogous to the reduction in the ESA of a probe beam that was observed in Ce:YAG as the crystal was cooled from room temperature to −20 °C.[6]

While it is proposed that the temperature effects reported here are directly related to the ESA transition, it is not known whether it is ESA or the resultant color centers that are more deleterious to laser performance. For example, it could be that at the elevated (multi kilohertz) PRFs of the frequency-doubled CVL that any color centers formed by the ESA transition do not have time to relax on the interpulse time scale. This might explain the increase in pulse energy observed when a chopper was used to reduce the pumping PRF, from 6.2 kHz to 30 Hz, of another frequency-doubled CVL-pumped Ce:LiLuF laser.[25] Additionally, this might be why other researchers who have operated lower (~10-Hz) PRF Ce:LiLuF lasers have not reported these temperature effects. However, the fact that we have thermally loaded our Ce:LiLuF laser far more severely than any other Ce:LiLuF laser reported to date (the highest ratio of pump average power to pump volume by a factor of 1000) could be the simple reason for the uniqueness of these observations.

5. Conclusion

The results of a number of investigations for further characterizing the effect of crystal temperature on the polarization characteristics of Ce:LiLuF lasers have been reported. In particular, laser experiments, pump–probe gain studies, and investigations into the effect of crystal temperature on fluorescence yield have been performed in an attempt to understand further the roles that color centers and ESA play in Ce:LiLuF. From our studies into Ce:LiLuF laser and gain performance in the vicinity of the predominantly σ-polarized 327-nm fluorescence spectrum peak, it was observed that the σ-polarized emission was characterized by higher small-signal gains and smaller laser pulse buildup times than the π-polarized emission. Indeed, in the absence of polarization selective cavity elements the laser oscillation was σ polarized. It is interesting, however, that the laser output power versus input power was found to be smaller and more saturated in the σ polarization than in the π polarization. To account for these anomalies, we conclude that ESA (and the associated formation of color centers) is more severe for σ-polarized lasing than for π-polarized lasing in this spectral region.

However, it is still not clear whether it is ESA or color-centre absorption that is the more serious impediment to Ce:LiLuF laser operation. Further pump–probe measurements are required to determine the relative magnitudes of the ESA and color-center absorption cross sections at the pump and laser wavelengths as well as the color centres' lifetimes. Investigations of higher-quality Ce:LiLuF crystals (which would reduce the probability of color-center formation but not of ESA) would also help to resolve this issue. Additionally, by using a chopper wheel to reduce the PRF of the frequency-doubled CVL and recording the color center induced absorption measured immediately after the crystal fluorescence as a function of the pump PRF, the color centers' lifetimes could be evaluated.

We postulate that, based on observations that crystal cooling led to enhanced laser performance and crystal fluorescence, crystal cooling results in a narrowing of the ESA absorption band, which reduces the probability of ESA and therefore of color-center formation. It is also tentatively suggested that the reason ESA and the effect of crystal cooling are more pronounced for σ-polarized emission than for π-polarized emission could be because the $5d \Rightarrow$conduction band energy is smaller perpendicular to the *c* axis than it is parallel to this axis.

Finally, given the marked improvements in Ce:LiLuF laser performance that we have observed with crystal cooling, it would be interesting to cool other cerium-doped materials that have demonstrated poor laser efficiency to date [such as Ce:YLF (Ref. 9) or Ce:LaF (Ref. 10)] or have not yet lased [such as Ce:YAG (Refs. 5–7 and Ce:CaF (Ref. 8] to determine whether crystal cooling could have a similar effect on these materials.

References

1. S. V. Govorkov, A. O. Weissner, T. Schroder, U. Stamm, W. Zschocke, and D. Bastings, "Efficient high average power and narrow spectral linewidth operation of Ce:LiCAF lasers at 1-kHz repetition rate," in *Advanced Solid State Lasers*, W. R. Bosenberg and M. M. Fejer, eds., Vol. 19 of OSA Trends in Optics and Photonics Series (Optical Society of America, Washington, D.C., 1998), pp. 2–5.
2. A. J. S. McGonigle, D. W. Coutts, and C. E. Webb, "530-mW 7-kHz cerium LiCAF laser pumped by the sum-frequency-mixed output of a copper-vapor laser," Opt. Lett. **24,** 232–234 (1999).
3. Z. Liu, K. Shimamura, K. Nakano, N. Mujilatu, T. Fukuda, T. Kozeki, H. Ohtake, and N. Sarukura, "Direct generation of 27-mJ pulses from a Ce^{3+}:$LiLuF_4$ oscillator using a large-size Ce^{3+}:$LiLuF_4$ crystal," Jpn. J. Appl. Phys. **39,** 88–89 (2000).
4. P. Rambaldi, R. Moncorgé, J. P. Wolf, C. Pedrini, and J. Y. Gesland, "Efficient and stable pulsed laser operation of Ce:$LiLuF_4$ around 308 nm," Opt. Commun. **146,** 163–166 (1998).
5. W. J. Miniscalco, J. M. Pellegrino, and W. M. Yen, "Measurements of excited-state absorption of Ce^{3+}:YAG," J. Appl. Phys. **49,** 6109–6111 (1978).
6. R. R. Jacobs, W. F. Krupke, and M. J. Weber, "Measurements of excited-state-absorption loss for Ce^{3+} in Y3Al5O12 and implications for 5*d*–4*f* rare earth ion lasers," Appl. Phys. Lett. **33,** 410–412 (1978).
7. D. S. Hamilton, S. K. Gayen, G. J. Pogatshnik, R. D. Ghen, and W. J. Miniscalco, "Optical-absorption and photoionization measurements from the excited states of Ce^{3+}:$Y_3Al_5O_{12}$," Phys. Rev. B **39,** 8807–8815 (1989).
8. G. J. Pogatshnik and D. S. Hamilton, "Excited-state absorption of Ce^{3+} ions in Ce^{3+}:CaF_2," Phys. Rev. B. **36,** 8251–8257 (1987).
9. D. J. Ehlrich, P. F. Moulton, and R. M. Osgood Jr., "Ultraviolet solid state Ce:YLF laser at 325 nm," Opt. Lett. **4,** 184–186 (1979).
10. D. J. Ehlrich, P. F. Moulton, and R. M. Osgood Jr., "Optically pumped Ce:LaF3 laser at 286 nm," Opt. Lett. **5,** 339–341 (1980).
11. M. A. Dubinskii, V. V. Semanshko, A. K. Naumov, R. Yu. Abdulsabirov, and S. L. Korableva, "Ce^{3+}-doped colquiriite, a new concept for all-solid-state tunable ultraviolet laser," J. Mod. Opt. **40,** 1–5 (1993).
12. C. D. Marshall, J. A. Speth, S. A. Payne, W. P. Krupke, G. J. Quarles, V. Castillo, and B. H. T. Chai, "Ultraviolet laser emission properties of Ce^{3+}-doped $LiSrAlF_6$ and $LiCaAlF_6$," J. Opt. Soc. Am. B **11,** 2054–2065 (1994).
13. J. F. Pinto, G. H. Rosenblatt, L. Esterowitz, and G. J. Quarles, "Tunable solid-state laser action in Ce^{3+}:$LiSrAlF_6$," Electron. Lett. **30,** 240–241 (1994).
14. M. A. Dubinskii, R. Yu. Abdulsabirov, S. L. Korableva, A. K. Naumov, and V. V. Semanshko, "A new active material for a solid state UV laser with an excimer pump," Laser Phys. **4,** 480–484 (1994).
15. N. Sarakura, M. A. Dubinskii, Z. Liu, V. V. Semanshko, A. K. Naumov, S. L. Korableva, R. Yu. Abdulsabirov, K. Edmatsu, and Y. Suzuki, "Ce^{3+} activated fluorides crystals as prospective active media for widely tunable ultraviolet ultrafast lasers with direct 10-ns pumping," IEEE J. Sel. Top. Quantum Electron. **1,** 792–804 (1995).
16. N. Sarukura, Z. Liu, S. Izumida, M. A. Dubinskii, R. Yu. Abdulsabirov, and S. L. Korableva, "All-solid-state tunable ultraviolet subnanosecond laser with direct pumping by the fifth harmonic of a Nd:YAG laser," Appl. Opt. **37,** 6446–6448 (1998).
17. A. J. S. McGonigle, D. W. Coutts, and C. E. Webb, "A 380-mW 7-kHz cerium LiLuF laser pumped by the frequency doubled

yellow output of a copper-vapor laser," IEEE J. Sel. Top. Quantum Electron. **5,** 1526–1531 (1999).
18. A. J. S. McGonigle, S. Girard, D. W. Coutts, C. E. Webb, and R. Moncorgé, "10 kHz continuously tunable Ce:LiLuF laser," Electron. Lett. **35,** 1640–1641 (1999).
19. P. Rambaldi, M. Douard, and J. P. Wolf, "New UV tunable solid-state lasers for lidar applications," Appl. Phys. B **61,** 117–120 (1995).
20. D. W. Coutts, "Optimization of line focusing geometry for efficiency nonlinear frequency conversion from copper-vapor lasers," IEEE J. Quantum Electron. **31,** 2208–2214 (1995).
21. D. W. Coutts and D. J. W. Brown, "Production of high average power UV by second-harmonic and sum-frequency generation from copper-vapor lasers," IEEE J. Sel. Top. Quantum Electron. **1,** 768–778 (1995).
22. J. Andreissen, H. Merenga, C. M. Combes, P. Dorenbos, and C. W. E. van Eijk, "Calculation of 4*f* and 5*d* energy levels of cerium in LiYF4 and LiLuF4 and LiBaF3, and estimate of local distortion," *in Proceedings of the International Conference on Inorganic Scintillators and Their Applications, 1995*, P. Dorenbos and C. W. E. van Eijk, eds. (Delft University Press, Delft University of Technology, Delft, 1996), pp. 142–143.
23. K.-S. Lim and D. S. Hamilton, "Optical gain and loss studies in Ce^{3+}:YLF_4," J. Opt. Soc. Am. B **6,** 1401–1406 (1989).
24. K.-S. Lim and D. S. Hamilton, "UV-induced loss mechanisms in a Ce^{3+}:YLF_4 laser," J Lumin. **40**/**41,** 319–320 (1988).
25. D. W. Coutts, J. S. Cashmore, and C. E. Webb, "Multi kHz PRF cerium lasers pumped by frequency doubled copper vapour lasers," in *Digest of the International Quantum Electronics Conference* (Optical Society of America, Washington, D.C., 1996), paper ThE3.